ELSEVIER

S0032-3861(96)00290-X

Polymer Vol. 37 No. 19. pp. 4257–4269, 1996

0032-3861/96/$15.00 + 0.00

Polymer solutions under elongational flow: 1. Birefringence characterization of transient and stagnation point elongational flows

D. Hunkeler*
Department of Chemistry, Swiss Federal Institute of Technology, EPFC-DC-IGC-I, CH-1015 Lausanne, Switzerland

and T. Q. Nguyen and H. H. Kausch
Polymer Laboratory, Department of Materials Science, Swiss Federal Institute of Technology (EPFL-MX-D), CH-1015 Lausanne, Switzerland
(Received 15 August 1994; revised 20 December 1995)

Birefringence measurements are reported in transient and stagnation point elongational flows created by forcing a polymer solution through a narrow contraction. A strongly molecular weight dependent birefringence was observed and attributed to segmental orientation caused by individual chain extension. The birefringence was also found to depend on the position within the flow field, the solvent type, thermodynamic quality and viscosity, the polymer composition, and the type of flow field. Two distinct concentration regimes, corresponding to the dilute and semi-dilute polymer regions, were observed. The transition was marked by a dynamic critical overlap concentration which was lower than that observed under quiescent conditions. In the dilute regime, a laminar flow profile was observed and intermolecular interactions were negligible. The modest local orientation and overall chain deformation however indicate that intramolecular hindrances to extension exist. Transient elongational flows were characterized by a 'tube-like' birefringence which had a diameter equal to that of the orifice and extended several orifice diameters into the solution. In contrast, stagnation point elongation flows possessed both the tube-like birefringence and the classical highly localized birefringent 'lines'. The transition between the tubular and linear birefringent zones is a function of the viscous coupling between the polymer coil and the deforming fluid element. This coupling is itself a complex function of temperature, molecular parameters and the flow conditions. Measurements in stagnation point elongational flows have also indicated that the maximum degree of local orientation does not occur at the stagnation point, and data indicate that chains continue to accelerate until a region very close to the orifice. In transient elongational flow the polymer dynamics follow a coil-to-deformed coil transition with birefringence saturation not observed. Copyright © 1996 Elsevier Science Ltd.

(Keywords: elongational flow; birefringence; polymer dynamics; coil-to-deformed coil)

INTRODUCTION

The flow-induced deformation of flexible polymer chains in solution can be observed whenever the polymer–solvent hydrodynamic drag forces overcome the random Brownian forces which tend to keep the chain in the coiled state. When this occurs, the statistical distribution of the polymer segments is distorted from the random state, and the optical property of the solution becomes anisotropic. This phenomenon, known as streaming birefringence or the Maxwell effect, provides important information on the state of local orientation of the molecular coil, and permits one to probe the process of chain unravelling in flow. Following the prediction of de Gennes[1] and the experimental work from Keller and Odell[2], it seems now to be well established that flexible chains in solution can become highly stretched or deformed under some special conditions of flow:

1. the flow must be persistently elongational, i.e. the extensional component must exceed the rotational component of the velocity gradient[3],
2. to overcome the Brownian forces, the product of the fluid strain rate ($\dot{\epsilon}$) and the longest relaxational time of

* To whom correspondence should be addressed

* Some authors[6] refer to the product $\dot{\epsilon}\tau$ as the Weissenberg number (We), with other authors suggesting that for We > 0.5 the flow becomes 'supercritical'[7]. The variance in the value of A reflects the different models used to predict polymer dynamics, and the uncertainty in the exact nature and magnitude of the coupling between the strain applied to the fluid element and the molecular strain imparted to the macromolecule. However, it is generally agreed[8] that the dimensionless parameter $\dot{\epsilon}\tau$ exceeds approximately unity then a condition for the sudden extension of the chain from a coiled to a 'stretched' state has been reached[2], and the chain deforms affinely with the fluid[9–11]. Recent unpublished data have found A to be between 5 and 14 for polystyrene in solvents of various thermodynamic quality[12]

the molecule (τ) must be larger than a critical value:

$$\dot{\epsilon}\tau > A \quad (1)$$

where A is a constant on the order of unity, which assumes slightly different values according to various authors[4,5]*.

3. the residence time of a fluid element in the high strain rate region (t), which is stream line dependent, must be much longer than the chain relaxation time (τ) in order for the embedded molecular coil to accumulate sufficient strain for the extension[4].

This last point constitutes the cornerstone in any theory dealing with molecular rheology and polymer dynamics. For stagnation point elongational flows these three conditions are satisfied for those streamlines passing through or very near to the stagnation point, and a coil-to-stretch transition has indeed been observed[2]. In contrast, elongational flows, created by forcing a liquid across a narrow contraction, have an inherent transient residence time which allows for only modest chain extension[3]. Nevertheless, flow birefringence is readily discerned in this type of flow, as shown by our present experiments, indicating a substantial degree of segmental orientation. The dependence of flow birefringence on the polymer molecular weight and concentration also reveals the existence of two different concentration regimes, corresponding to the dilute and the semi-dilute regimes.

At strain rates exceeding those required to elongate a polymer coil, the thermomechanical process of energy transfer from the fluid to the chain begins to reduce the bond dissociation energy and cause chain fracture. Therefore, the study of mechanochemical degradation[13], apart from being interesting in its own right, will also permit us to probe the non-equilibrium conformation of molecular coils during fast chain unravelling and to determine if polymers can be degraded in flow under a partial state of chain uncoiling.

EXPERIMENTAL

Birefringence observations

Flow visualization, birefringence and degradation measurements were performed using a single-jet cell, shown schematically in *Figure 1* and an opposed jet apparatus similar to that of Farrell *et al.*[14]. The

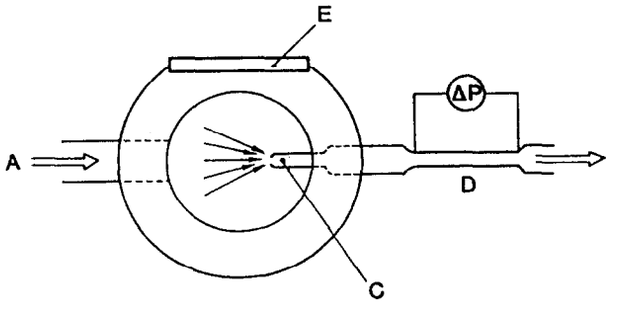

Figure 1 Schematic view of a single-jet cell used for birefringence, degradation and flow visualization experiments

elongational flow field was created by pumping the polymer solution, at a controlled flow rate, across an abrupt contraction (0.4 mm internal diameter). In some experiments pressure transducers were added after the solution passed through the jet(s) and the signal was used to monitor the flow rate in an on-line manner. The optical train used for birefringence observation has been schematicized in a previous publication[13]. Monochromatic light (632.8 nm) was emitted by a 6 mW HeNe laser (Spectra Physics Model 120S). The light was passed through a dichroic glass type 4K polarizer (Spinnler and Hoyt), oriented at 45° with respect to the flow direction, and focused by a microscope objective to the region in front of the orifice entrance. It then passed through an analyser oriented at 90° with respect to the first polarizer before being collected with a condensing lens onto a silicon photodiode (Hamamatsu, model S3887). To compensate for residual birefringence from the glass windows, a zero-order temperature compensated quarter-wave plate (Optics for Research) was inserted in front of the cell with its slow axis parallel to the polarizer (Senarmont compensator). This greatly improved the extinction (dark field) that was obtainable. The entire cell was attached to a two-dimensional micropositioner which allowed the optical axis to be translated across the jet in a direction parallel (x-axis) or perpendicular (y-axis) to the flow velocity. This allowed for an adjustment with a precision of 10 μm. The focused beam diameter (d_f) at the orifice entrance was equal to 0.05 mm as was determined by the following relation:

$$d_f = (4/\pi)(\lambda f/d) \quad (2)$$

where λ is the laser wavelength (632.8 nm), f the focal length of the microscope objective (50 mm) and d the laser beam diameter (0.8 mm at half intensity).

Flow visualization

The visualization of transient elongational flows was made possible through the addition of a third cell window at the top of the single jet apparatus (*Figure 1*). This enabled photographs to be taken perpendicular to both the flow and optical axis. The streamlines were photographed by orienting an Olympus model SZ stereoscopic microscope with a photographic adapter (PM) and automatic exposure control (PM10-AD) at 90° with respect to both the flow direction and the optical train axis. A narrow region of the flow field was illuminated by means of a cylindrical lens placed directly in front of the cell which produced a sheet of light. The horizontal and vertical location of the light sheet could be adjusted using two-dimensional micropositioners with a precision of ± 10 μm. The flow field was visualized using tracer particles such as nascent polyethylene or milk latex. However, in most cases such large scattering bodies were unnecessary and the streamlines were easily delineated from the light scattered by the residual dust from a twice clarified aqueous solution. In this respect birefringence measurements are much more convenient than light scattering, particularly for high molecular weight water soluble polymers, since the trace residuals of dust are difficult to completely remove without affecting the mass concentration of the polymer in the sample. Photographs were taken at different horizontal positions from the jet. The vertical position was maintained at the centre of the axis, where birefringence

and elongation are maximized.

High speed Polariod 'Professional' film (type 667, 3000 ASA) was used to record the scattering images. In some instances longer exposures were recorded on 80 ASA type 665 film.

Flow field modelling

Flow field simulations of dilute polymer solutions were performed using POLYFLOW (Polyflow S.A., Louvain-la-Neuve, Belgium) a finite element program dedicated to Newtonian and viscoelastic fluids. For our purposes fluid incompressibility was assumed and the inviscid approximation employed.

Degradation experiments

Polymer solution degradation experiments were performed in both the single jet and opposed jet apparatuses. The polystyrene (PS) or poly(ethylene oxide) (PEO) solutions were pumped using a Watson-Marlow Model 2601V/R168 peristaltic pump (Roto-Consulta, Switzerland) from a collection reservoir which was isolated from the atmosphere. The polymer solution then passed sequentially through a pulse dampener, the flow cell, the on-line pressure transducers and into a collection reservoir. The solutions were virgin polymers prepared on the same day as the experiment, and were not recycled. In order to obtain samples for chromatographic characterization the flow was first allowed to equilibrate, as measured by the stabilization of the pressure drop across the transducers, and then the first 100 ml of solution was discarded. A prewashed sample bottle was then added at the end of the flow line and the polymer solution collected. The flow rate was subsequently changed, the system allowed to re-equilibrate, and an additional sample taken. This cycle was repeated for each measured strain rate. During all experiments the flow rate history was increasing with time so as to allow samples of polymers exposed to the lowest strain rate to be collected first.

Following the sample collection, the solvent (decalin for PS) was evaporated in a Büchi EL131 rotary vacuum distillation apparatus. The polymer residue was subsequently redissolved in tetrahydrofuran (Fluka A.G., puriss pro analysi, >99.5%) and diluted to a concentration such that the product $[\eta]c$ was less than 0.025. The sample was subsequently injected into a Waters 150C gel permeation chromatograph (g.p.c.) for molecular weight determination. The instrument was equipped with a variable wavelength ultraviolet detector (Perkin Elmer 75C) and was modified to permit data acquisition on a PC-AT compatible computer. Two ultrastyragel columns were used in series ($2\ 10^6$ Å and 10^5 Å). Molecular weight distributions were collected and interpreted using 'Multidetector GPC Software, Version 2.20'[15].

Chemicals

PS standards were obtained from Polymer Laboratories (Shropshire, UK). The polystyrenes had molecular weights of 4.00×10^6 ($\overline{M}_w/\overline{M}_n < 1.04$) and 8.50×10^6 ($\overline{M}_w/\overline{M}_n < 1.20$). PEO samples with a broad molecular weight distribution (PDI > 5) were obtained from Union Carbide (Geneva, Switzerland). PEO solutions were prepared with pre-clarified water. The double distilled water was prepared on a quartz 'Fi-stream' still manufactured by Fisons. It was then passed through a Millipore Milli-Q system of four cartridges with the last unit containing a 0.22 μm membrane filter. The polymer solutions were passed through a high porosity glass filter (40–100 μm) to avoid degradation.

Decalin was obtained from Fluka A.G. (Switzerland) with a purity exceeding 98% and a composition of 41% *cis*, 58% *trans*-decahydronaphthalene and 1% tetrahydronaphthalene as determined by gas chromatography. It was used without further purification.

Theory of flow birefringence

The light intensity of the detected signal (I_s) is given by:

$$I_s = I_o \sin^2 2\theta \sin^2(\delta/2) \quad (2)$$

where θ ($= \pi/4$) is the orientation of the principal axis of the refractive index with respect to the incident polarization vector, and I_o is the incident beam intensity. The quantity δ is the average retardation angle (equation (5)) and is related to the birefringence, Δn ($= n_{||} - n_{\perp}$), as:

$$\Delta n = (\lambda\delta)/(\pi z) \quad (3)$$

where z is the path length (approximately one orifice diameter, or 0.4 mm). For the high molecular weight solutes used in this elongational flow investigation, form birefringence was negligible compared with intrinsic birefringence. For small phase differences the following approximation is valid:

$$I_s = (I_o\delta^2/4) \quad (4)$$

This equation shows that the intensity varies as the square of the retardation with such detection said to be quadratic. From equation (4), it is clear that the local birefringence of the polymer solution cannot be determined directly from the retardation measurement due to inhomogeneities in the flow field (*Figure 2*). The measured retardation $\delta(y)$ is however related to the birefingence Δn, which is an axisymmetric function of the radial distance r:

$$\delta(y) = (2\pi/\lambda)\int_{-\infty}^{+\infty} \Delta n(r)dz$$

$$= (4\pi/\lambda)\int_{y}^{+\infty} \Delta n(r)rdr/(r^2 - y^2)^{1/2} \quad (5)$$

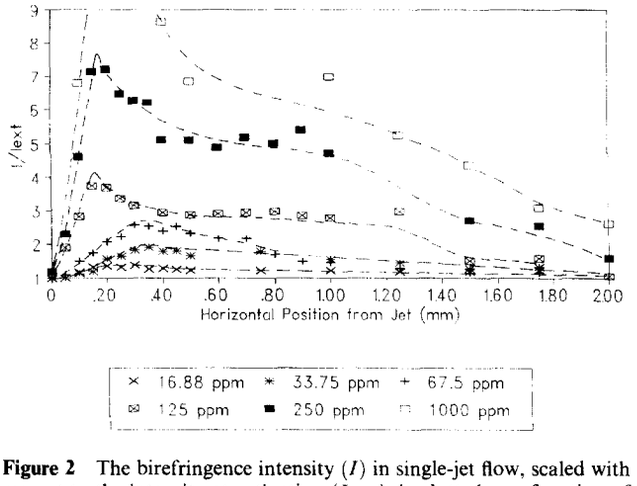

Figure 2 The birefringence intensity (I) in single-jet flow, scaled with respect to the intensity at extinction (I_{EXT}), is plotted as a function of the horizontal distance (mm) from the jet. The horizontal refers to the axis collinear with the elongational flow. Measurements were performed on a PEO with a molecular weight ($\overline{M}_w$) of 4×10^6. Polymers were dissolved in water at concentrations of 16.875, 32.75, 67.5, 125.0, 250, 500 and 1000 ppm

Experimentally, it has been found that the retardation curve $\delta(y)$ (obtained by taking the square root of the signal from an intensity signal such as is shown in *Figure 2*) is reasonably well approximated by a Gaussian shape. In this case, the birefringence function can be solved analytically from equation (6) with an inverse Abel transformation[16], giving a Gaussian distribution function similar in shape to $\delta(y)$. In this work birefringence was measured exclusively using the intensity method since it yielded more precise data than observations based on the extinction angle.

RESULTS AND DISCUSSION

Transient elongational flow

A polymer in solution can exist as an isolated molecule or as an entangled network, depending on the degree of coil interactions[17]. The formation of a topological network is believed to occur after extensive molecular overlap, generally at a concentrations much higher than c^*. For the PEOs used in the present experiments, it was determined from the reported molecular weights that c^* under dynamic flow conditions is approximately 140, 170 and 250 ppm for the 7×10^6, 4×10^6 and 2×10^6 dalton samples respectively. These values are much below the corresponding critical overlap concentration in quiescent conditions ($c^* = 3500$, 4500, 6500 ppm). In *Figure 3* two birefringence regimes are indeed observed. This change in the solution behaviour with concentration has also been recently observed by Hasegawa and Nakamura[18] and Kramer and Hoffmann[19], who respectively investigated the elongational flow of coiled and rigid rod polymers. The determined threshold values are smaller than c^*, indicating that molecular coils start to overlap at a much lower value of the concentration when under a persistently elongational flow. Nguyen and Kausch also reported similar effects in transient elongational flows[13]. Keller, Odell and Miles explained this in terms of the time scale for intermolecular entanglement formation[20]. In this work the critical polymer concentration for the onset of network formation was found to decrease with the polymer molecular weight ($C \propto M^{-0.47}$) in qualitative agreement with the critical overlap concentration under quiescent conditions.

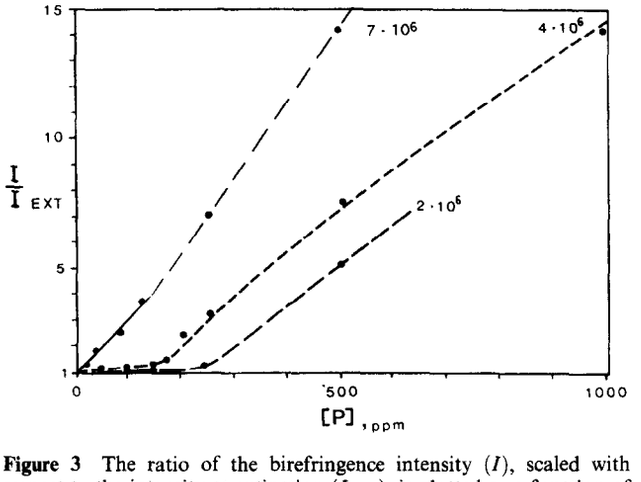

Figure 3 The ratio of the birefringence intensity (I), scaled with respect to the intensity at extinction (I_{EXT}), is plotted as a function of the concentration of polymer for PEO samples of different molecular weights

Figure 2 shows birefringence profiles for a PEO with a M_W of 4×10^6. The birefringence is observed to be position dependent with a maximum very close to the orifice. The birefringence intensity decreases as the horizontal distance from the jet increases. The plateau at 0.5–1 mm from the orifice is believed to be due to the heterogeneity of the molecular weight distribution. From *Figure 2* it is evident that for polymer concentrations well below the semi-dilute regime a strong birefringence intensity is still evident. Indeed, birefringence is observed at concentrations as low as 16 ppm. We can therefore conclude that for solutions well below the dynamic overlap concentration ($c \ll c^*_{dynamic}$) the observed birefringence is due to segmental chain orientation and intermolecular entanglement effects are negligible.

Figure 4 shows a plot of the velocity and strain rate in the vicinity of a 1.0 mm orifice simulated by

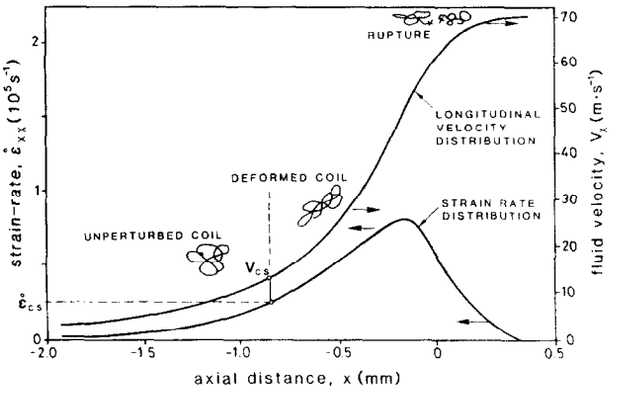

Figure 4 Strain rate and fluid velocity as a function of the position from the orifice as calculated by POLYFLOW. The orifice diameter was 1.0 mm in the simulation

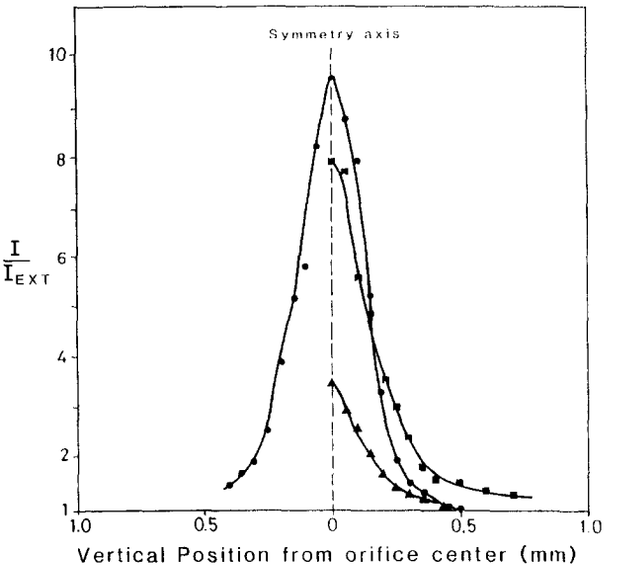

Figure 5 The birefringence intensity (I), scaled with respect to the intensity at extinction (I_{EXT}), is plotted as a function of the vertical distance from the centre of the orifice. Measurements were performed on a 1000.0 ppm solution of PEO in water with a molecular weight of 4×10^6. The full profile (●) was recorded at a horizontal position 350 μm from the jet. The two half profiles were recorded 450 μm (■) and 500 μm (▲) from the jet respectively

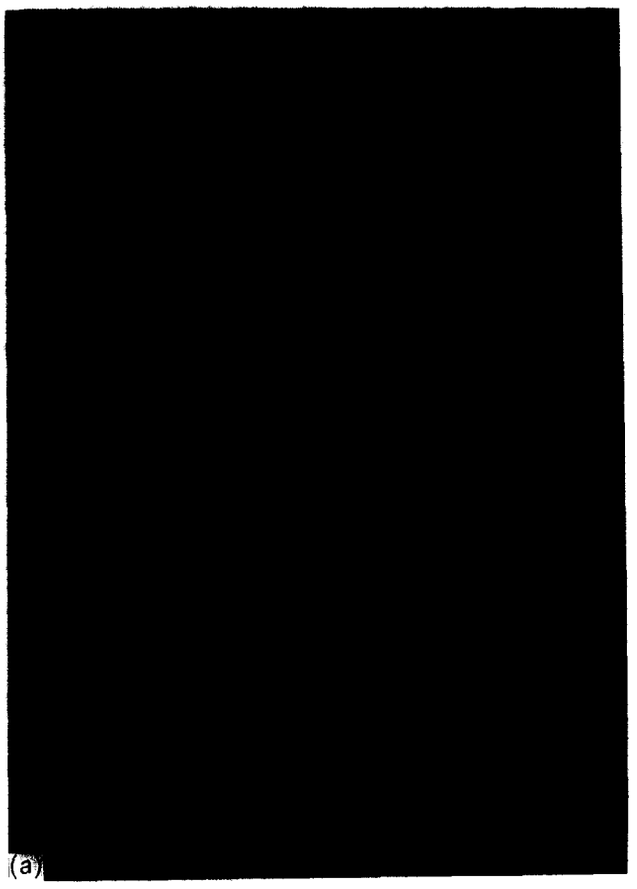

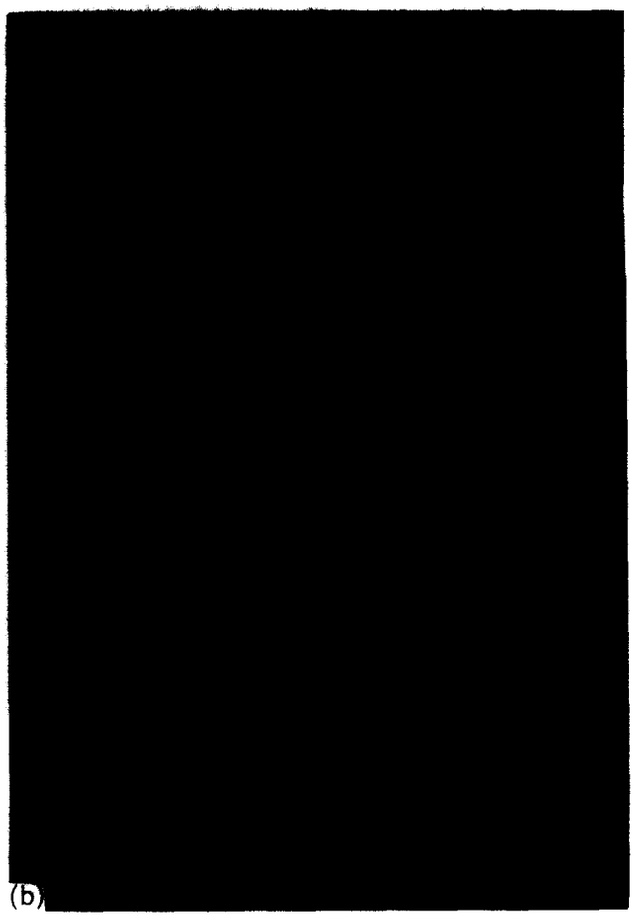

POLYFLOW. Given that the deformation (birefringence) is related to the applied strain rate, the predictions of POLYFLOW are in remarkable qualitative agreement with the birefringence measurements. Both indicate a highly localized region of chain extension within one orifice diameter of the abrupt contraction (*Figure 2*) followed by a transition to less extended molecules further from the orifice entrance. These results also agree very well with Armstrong *et al.*'s simulation[21] which shows a strain rate function with a maximum close to the front of the orifice.

Vertical profiles have also been observed (*Figure 5*) with a maximum coincident with the streamline passing through the centre of the flow axis. The shape of these profiles is very similar to that recently reported by Cathey and Fuller[16] and Menasveta and Hoagland[22]. Furthermore, our vertical profiles have diameters corresponding to the width of the orifice (0.4 mm). This birefringence zone can be visualized with an optical photomicrograph of a 100 ppm PEO solution (*Figure 6*) which indicates the 'tube like' character of this strong transient elongational flow, and the correspondence of the tube size with the radius of the orifice. Cathey and Fuller[16] have also observed vertical birefringence profiles very similar in diameter to their orifice. These observations indicate that in fast transient flows of PEO the birefringence is spread over a large volume (tube) in contrast to the highly localized 'birefringent lines' observed for the quasi-stationary state flow of PS solutions[23]. The nature of the discrepancy in these results can be attributed either to a difference in the polymer composition (ethylene oxide *versus* styrene) or flow type, and will be discussed in detail in a subsequent section of this paper. The height of the vertical profile decreases as either the flow rate decreases (*Figure 7*) or the horizontal position from the jet increases (*Figure 6*), both of which correspond to a decrease in the energy transmission from the bulk fluid to the macromolecules. A decrease in birefringence with flow rate has previously been observed by both Keller and Odell[2] and Farinato[24] for the quasi-stationary state flow of PS and polyacrylamide solutions respectively.

It is important to note that our tube-like birefringence is not due to pipe or flare phenomena as suggested by Chow *et al.*[25], but rather due to individual chain extension. *Figure 4* in Chow's paper shows the elongational flow behaviour of PS solutions. Our experiments, at all polymer concentrations and strain rates, lie in the 'stretch' regime, well below both the pipe and flare domains. For PEO, our experiments at very low polymer concentrations (dilute regime) are also in the stretch

Figure 6 (a) Optical photograph of a 100.0 ppm solution of PEO in water with a molecular weight of 4×10^6. This transient elongational flow experiment was performed at a strain rate of $2.12 \times 10^4\ s^{-1}$ and recorded on 3000 ASA Polaroid film with an exposure time of 1.0 s. The 'tube' like character of the birefringence is evident. (b) A photograph of a 100.0 ppm solution of PS in decalin in the presence of a transient elongational flow field is shown. The polymer had a molecular weight of 4.00×10^6 daltons. The experiment was performed at a strain rate of $7.55 \times 10^4\ s^{-1}$ and recorded on 3000 ASA Polariod film with an exposure time of 1.0 s. The 'tube' like character of the birefringence is evident in contrast to the narrow birefringence 'lines' observed for PS–decalin by Keller and Odell[2] and also in this work (*Figure 17*) for a stagnation point elongational flow field

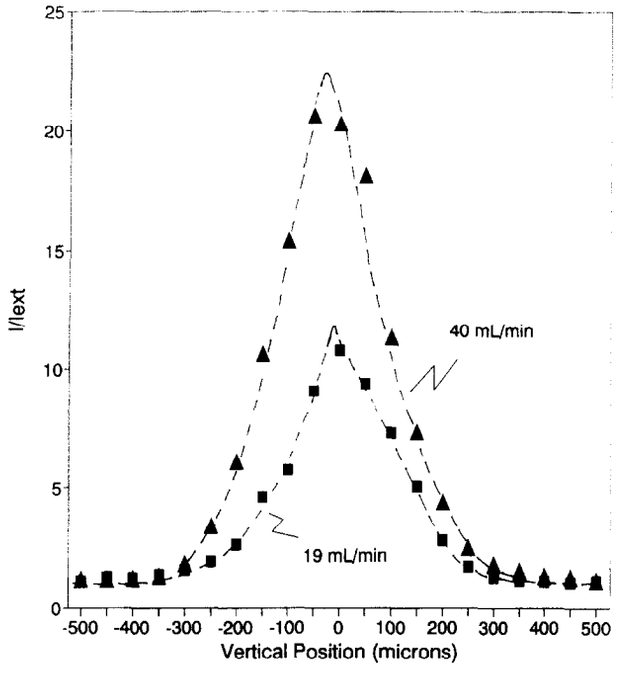

Figure 7 Birefringence intensity profiles (I), scaled with respect to the intensity at extinction (I_{EXT}), are plotted as a function of the vertical distance from the centre of the orifice. Measurements were performed on a 1000.0 ppm solution of PEO in water with a molecular weight of 4×10^6. The profiles were recorded at flow rates of 40 and 19 ml min^{-1} respectively which corresponds to strain rates of 1.49×10^4 and 0.71×10^4 s^{-1}. Measurements were taken at a horizontal position 400 μm from the jet

domain (*Figure 3* of Chow *et al.*[25]). The photograph in *Figure 8* shows a 1000 ppm PEO solution. This concentration is in the semi-dilute region and the birefingence zone extends several orifice diameters away from the jet ($\approx$ 2 mm) due to intermolecular entanglements of the polymer chains ($c^* > c^*_{dynamic}$). The extension of the birefringence zone with increasing polymer concentration is also seen in the horizontal profiles in *Figure 2*.

In a theta solvent the width and height of the birefringence zone are observed to decrease to about two-thirds the magnitude in a thermodynamically good solvent indicating that energy transmission from the bulk flow to the chain is less efficient in a more compact state (*Figure 9*). Cathey and Fuller have also reported that the shape of the birefringence zone is the same in both good and theta solvents[16].

Figure 10 shows the birefringence-strain rate plot for 100 and 1000 ppm PEO solutions with a M_W of 4×10^6. The position of maximum strain rate was predetermined by performing both horizontal and vertical scans about the orifice. The data show a critical strain rate for the coil-to-deformed coil transition of 3000 s^{-1}. The strain rate was obtained for the maximum strain rate along the central stream line for an abrupt contractional flow from the relation $(\dot{\epsilon}) = 0.56\,Q/(\pi r_0^3)$, where Q is the flow rate. We can conclude from *Figure 10* that extension or deformation are clearly observed but saturation is not evident. An absence of saturation has been recently reported in the elongational flow of rigid molecules such as methyl cellulose triacetate[26] and hydrolysed polyacrylamide[27]. Furthermore, Peterlin[28], Smith *et al.*[29] and Menasveta and Hoagland[22] have investigated the transient and stagnation point elongational flow behaviour of polyisobutylene, cellulose nitrate and PS molecules respectively. All authors reported bulk chain deformation much less than would be expected for a fully extended chain. Therefore, for fast transient flows we can conclude that both local orientation and global deformation are *not* saturated at values of the strain rate that have been experimentally observed. In quasi stationary state flows, birefringence has been reported to saturate[16,22,30], however, the overall deformed length, as measured by light scattering, is certainly much less than can be interpreted as due to a full chain extension[22]. This apparent disparity in the behaviour of stagnation point and transient flows will be discussed in a subsequent publication[31].

Measurements of PEO in transient flows at different molecular weights indicate that the critical strain rate for the coil-deformed coil transition scales approximately with the molecular weight to the -1.81 power, based on data for which no polydispersity correction was performed. This agrees with recent observations in stagnation point elongation flow (Atkins *et al.*[32]: -1.85 based on three measurements of fairly polydisperse pullulan polysaccharides, Nguyen *et al.*[12]: -1.77/-1.82 for polystyrene in methyl naphthalene and toluene respectively) and theoretical models for non-free draining coils (Kirkwood–Riseman–Zimm[33,34]) which predict a -1.767th order for good solvents

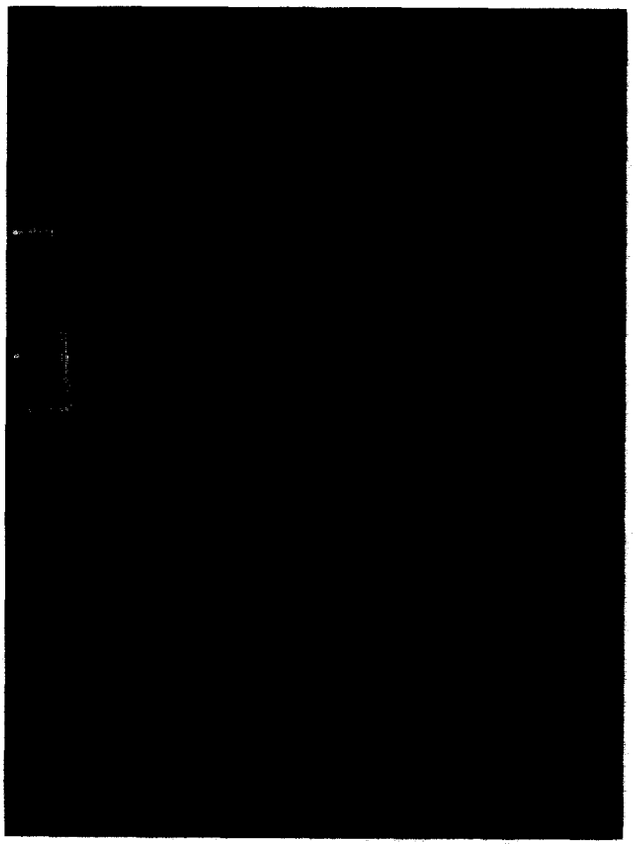

Figure 8 Optical photograph of a 1000.0 ppm solution of PEO in water with a molecular weight of 4×10^6. The experiment was performed at a strain rate of 1.24×10^4 s^{-1} and recorded on 3000 ASA Polaroid film with an exposure time of 8.0 s. The birefringence 'zone' is observed to extend for several orifice diameters away from the jet. This is caused by intermolecular entanglements which are characteristic of polymer chains in the semi-dilute regime

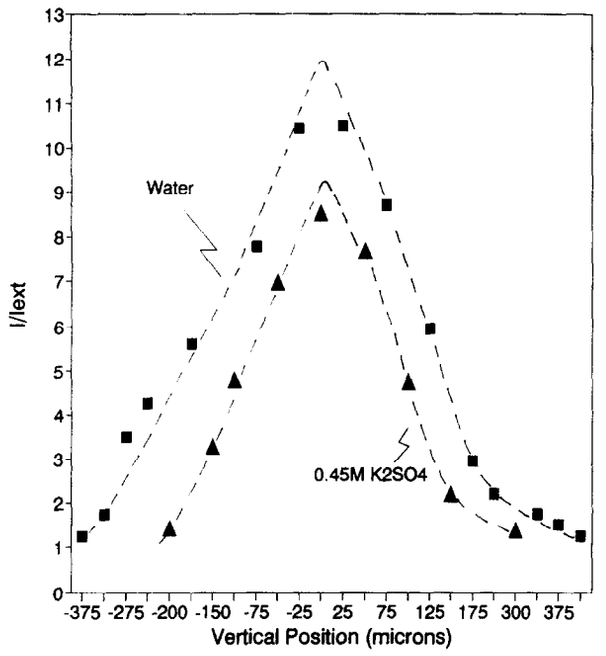

Figure 9 Birefringence intensity profiles (I), scaled with respect to the birefringence intensity at extinction (I_{EXT}), are plotted as a function of the vertical distance from the centre of the orifice. Measurements were performed on a 1000.0 ppm solution of PEO with a molecular weight of 4×10^6. Two profiles are shown corresponding to measurements in a thermodynamically good solvent (water, ■) and a theta solvent (0.45 M K_2SO_4, ▲). The profiles were recorded at a flow rate of 28.6 ml min^{-1} respectively which corresponds to a strain rate of 1.06×10^4 s^{-1}

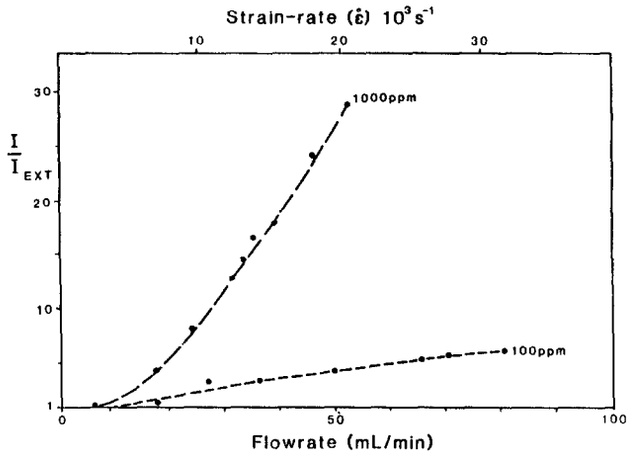

Figure 10 Birefringence intensity measurements (I), scaled with respect to the birefringence intensity at extinction at intensity (I_{EXT}), are plotted as a function of the applied strain rate. Data are for a PEO with a molecular weight of 4×10^6 dissolved in water at concentrations of 100 and 1000 ppm. The data show a lack of birefringence saturation as a function of the applied strain rate

($\tau \sim M^{3\nu} \sim 1/\dot{\epsilon}, \nu = 0.5$ in theta solvents and 0.589 in good solvents)†. It is our belief that this 'coil-to-stretch' transition more appropriately represents a coil-to-deformed coil progression since collective segmental orientation is observed in the absence of significant chain extension. Irregardless of the nomenclature such a transition has not been previously observed in a transient flow field, although measurements have been reported in stagnation point elongational flow and simple shear arrangements. This observation, coupled with previous results[16,35], indicates that a transient flow field locally orients the polymer chains. Furthermore, after the volume element around the coil has accumulated sufficient energy from the applied strain, a precise midchain scission is observed beyond a strain rate exceeding the critical value for fracture ($\dot{\epsilon}_f$)[36]. The molecular weight dependencies of the critical strain rates for the coil-deformed coil transition and chain

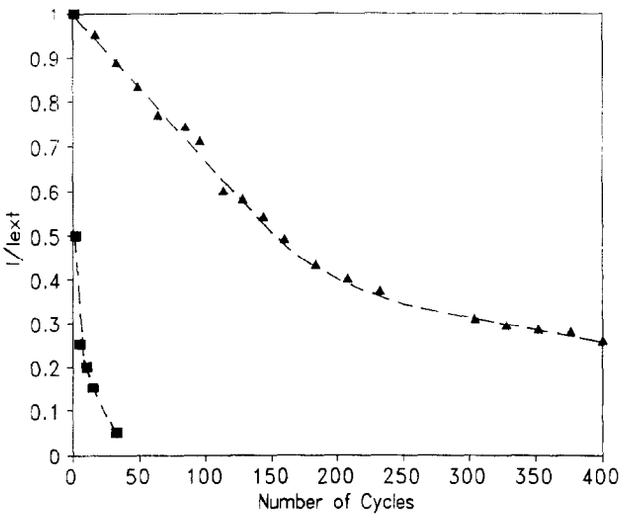

Figure 11 Birefringence intensity measurements (I), scaled with respect to the birefringence intensity at extinction at intensity (I_{EXT}), are plotted as a function of the number of times a virgin polymer solution has been recycled through the flow apparatus. Data are for a PS with a molecular weight of 4.00×10^6 ($\overline{M}_w/\overline{M}_n < 1.04$) dissolved in decalin at a concentration of 1000 ppm. The data show a reduction in the birefringence intensity with the number of times a solution was recycled, indicating that a fraction of the chains are degraded with each pass through the apparatus. It is also evident that the degradation is much more favourable in transient flows (single jet, ■) than stagnation point flows (opposed jets, ▲). The strain rate was maintained at 2.12×10^4 s^{-1} through each jet for the duration of the experiment

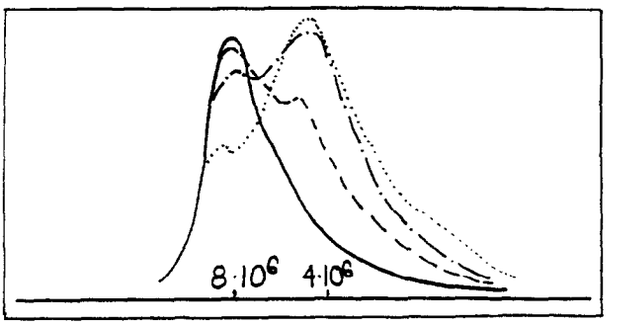

Figure 12 G.p.c. traces of a PS with a molecular weight of 8.5×10^6 ($\overline{M}_w/\overline{M}_n > 1.20$) prior to and after degradation caused by transient elongational flow through the single jet apparatus. The curves correspond to an undegraded polymer (——) and solutions exposed to shear rates of 2.12×10^4 s^{-1} (- - -), 3.24×10^4 s^{-1}(– · –) and 3.73×10^4 s^{-1} (· · ·) respectively. The degradation is observed to increase with the applied strain rate. The non-random midchain nature of chain scission is also evident

† It is important to note that experimental observations by Odell and Keller indicate that $\dot{\epsilon} \sim M^{-1.5}$, independent of the solvent quality. Indeed this scaling dependence is believed to be so universal that Odell and Keller have used it to develop an instrumental method for the measurement of the molecular weight distribution based on birefringence. Therefore, while the relationship $\tau \sim M^{3\nu}$ is certainly correct the reciprocal relationship between $\dot{\epsilon}$ and $1/\tau$ may be doubtful based on the accumulated experimental evidence

fracture will be used to evaluate models of polymer dynamics in the next paper in this series[31].

Figure 11 shows a reduction in the birefringence intensity with the number of times the polymer solution was recycled. This indicates chain scission is proceeding and the degraded lower molecular weight products are less susceptible to the strain rate and show a lower degree of segmental orientation. G.p.c. measurements on PS have confirmed the very efficient degradation of polymer chains in transient elongation flows (*Figure 12*)[36], and show the dependence of fracture on the applied strain rate. When this propensity for scission is coupled with the lack of birefringence saturation, evident in *Figure 10*, one can conclude that dilute solutions of polymer chains in transient elongational flows are not fully extended and are just deformed prior to fracture. This supports the results of Smith *et al.*[29] who found an increase in the radius of gyration by only a factor of 4, compared to the unperturbed dimension, in a transient elongational flow.

Figure 13b shows the streamlines for a 100 ppm solution of PEO with a molecular weight of 4 million. *Figure 13b* is a composite drawing traced from four individual photographs at different horizontal positions, an example of which is shown in *Figure 13a*. These photographs and images represent experiments carried out in transient flow at concentrations below the critical overlap concentration. The streamlines with added polymer are the same as were observed in pure water under identical conditions. This indicates that the polymer is not interfering with the flow field, as was also observed by Odell and Keller[2] in stagnation point elongational flows, and turbulence is *not* observed. Since the polymer concentration is less than the overlap concentration under dynamic conditions, then the birefringence and segmental orientation are due to individual chain extension and *not* the formation of

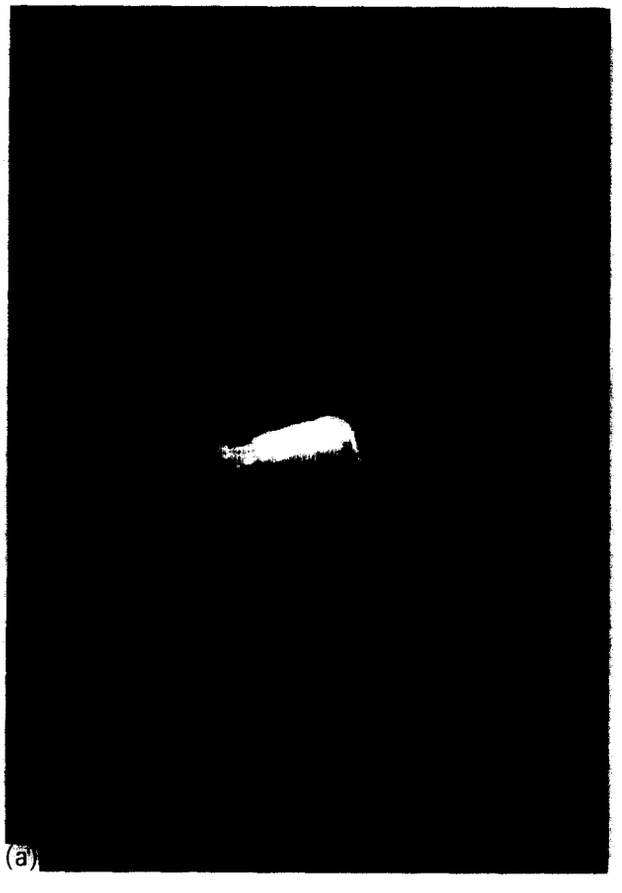

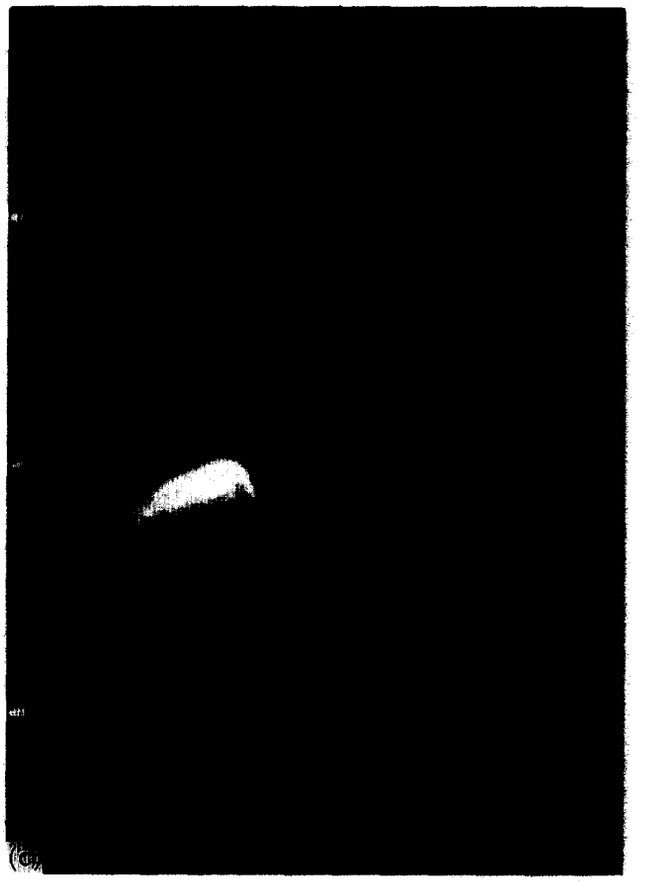

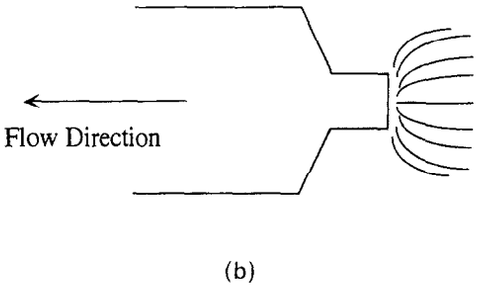

(b)

Figure 13 Optical photographs of the streamline flow pattern in the transient elongational flow of PEO in water. These images were recorded on a 100 ppm solution of PEO with a molecular weight of 4×10^6. The experiments were conducted at a strain rate of $2.12 \times 10^4\ s^{-1}$: (b) is a composite sketch which was traced directly from four individual photographs, such as is shown in (a); (c) is a photograph of the same PEO at 1000 ppm and a strain rate of $1.24 \times 10^4\ s^{-1}$

topological networks. Further, the observed degradation is not due to turbulence or intermolecular interactions. In contrast to the preceding results, PEO solution was photographed in the semi-dilute regime (*Figure 13c*) and shows characteristics of flow turbulence. Based on the series of photographs, we can conclude that turbulence and/or topological network formation are only observed in fast transient flows in the semi-dilute regime.

Stagnation point elongational flow

For the elongational flows investigated herein the birefringence has been observed to depend on the chemical composition of the polymer. For PEO, stagnation point and transient elongational flows are identical with the birefringence-strain rate curves superimposable as is shown in *Figure 14*. In such experiments, conducted in the opposed jet cell, each jet acts independently with the birefringence-zone equal to the diameter of the orifice. However, in contrast to the situation in transient elongational flow, the zone does not extend over a large distance because it is hindered by the second, or opposed, jet. Therefore, contrary to the classical interpretation of elongational flows where a stagnation point flow possesses essentially infinite strain for streamlines at the stagnation point, the transient flows have much lower strains, it seems from these observations that the residence time in the strong flow region in transient flows exceeds that for stagnation point flows (for PEO). A discussion of the differences between quasi-stationary state flows and fast transient flows will be discussed in a subsequent publication[31].

Poly(ethlyene oxide). From *Figure 15* the maximum birefringence, and chain extension, are observed to occur close to the orifice jets. At the stagnation point (centre of the two jets) the birefringence is near unity, indicating a very modest level of segmental chain orientation. The data, which indicate two non-overlapping birefringence tubes, are supported by the optical photograph of *Figure 16*. The birefringence zone also extends a much smaller distance from the orifice than in the single-jet apparatus (*Figure 8*).

Polystyrene. The PEO data in the preceding paragraph are in stark contrast to what is observed for PS in decalin

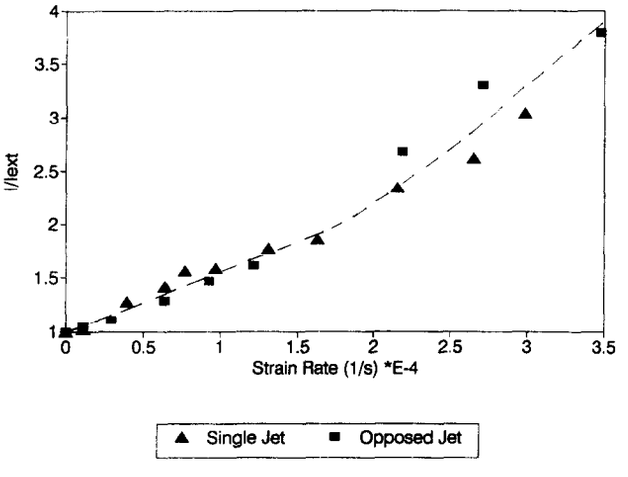

Figure 14 Birefringence intensity measurements (I), scaled with respect to the birefringence intensity at extinction at intensity (I_{EXT}), is plotted as a function of the applied strain rate. Data are for a PEO with a molecular weight of 4×10^6 dissolved in water at a concentration of 100 ppm. The data do not show a significant difference between measurements in transient (▲) and stagnation point (■) elongational flows

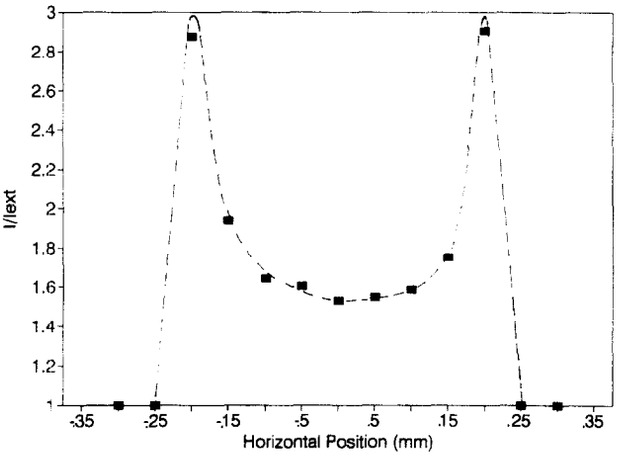

Figure 15 The birefringence intensity (I), scaled with respect to the birefringence intensity at extinction (I_{EXT}), is plotted as a function of the horizontal distance (mm) from the midpoint of the opposed jets. Experiments were performed on a PEO solution with a molecular weight of 4×10^6 in a stagnation point elongational flow. Polymers were dissolved in water at a concentration of 1000 ppm

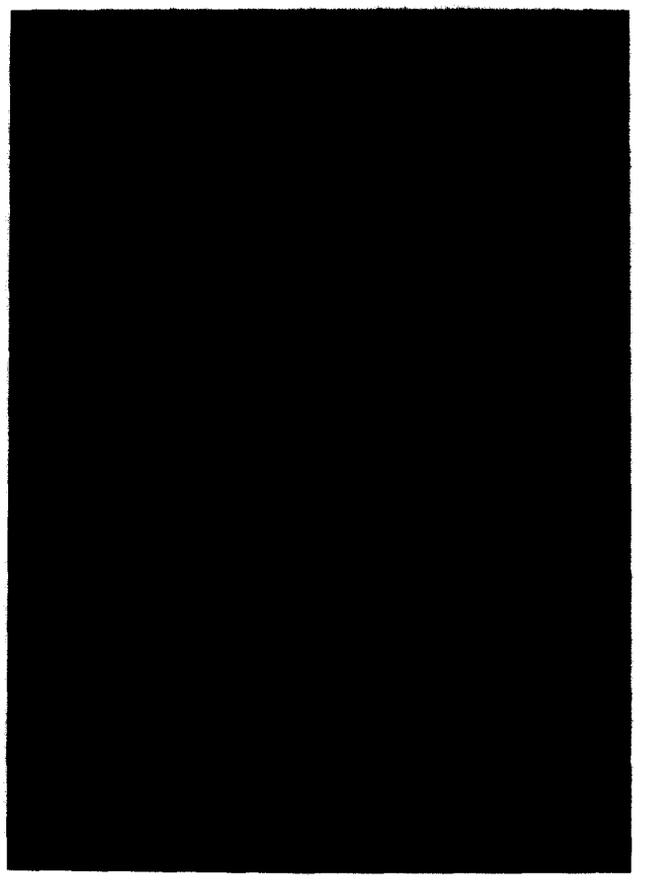

Figure 16 An optical photograph of a 1000 ppm solution of PEO in water with a molecular weight of 4×10^6 is shown. This stagnation point elongational flow experiment was performed at a strain rate of $1.24 \times 10^4\ s^{-1}$ and recorded on 3000 ASA Polaroid film with an exposure time of 1.0 s

where the opposed jet apparatus creates a narrow highly localized 'birefringence line' which has a volume two-orders of magnitude (53×) smaller than the birefringence 'tubes' observed in transient elongational flows (*Figure 17*). Such birefringence lines are similar to those observed by Mackey and Keller[23] and Odell and Keller[2,30] for polyethylene and PS systems respectively. The differences between stagnation point and transient elongational flow of polystyrene solutions are revealed in the vertical profiles of *Figure 18*. The birefringence intensity is clearly much stronger and more localized for a stagnation point flow. In stagnation point flows a narrow line, with a diameter of approximately 0.1 mm, is formed where the chains are highly extended. Outside this region, although still within the diameter of the orifice, the chains are essentially unperturbed. In contrast, transient flows impart energy to a larger number of molecules over a greater volume. This agrees with the optical photographs of *Figures 6b* and *17* which image birefringence tubes and lines respectively.

In the horizontal profile (*Figure 19*) a maximum is observed near the orifice and this decays only slightly between the two jets. It is interesting to note that the maximum in the birefringence signal is *not* observed at the stagnation point‡. The strong birefringence extending over the entire horizontal separation of the opposed jets, and the sharp vertical profile in *Figure 18*, provide a quantitative explanation for the existence of the narrow birefringent lines photographed in *Figure 17*. This is markedly different from the situation for PEO where the birefringence has a very reduced magnitude at the stagnation point (*Figure 15*), the vertical profile extends over the entire radius of the jet (*Figure 5*), and a tube like birefringence is observed (*Figure 16*).

The dependence of the birefringence intensity on the applied strain rate is shown in *Figure 20* for PS–decalin under transient and stagnation point elongational flows. While the PS deforms at the same critical strain rate in both types of flows, the magnitude of the birefringence is much larger in stagnation point flows relative to transient conditions. This is similar to the vertical profiles shown in *Figure 18*. Furthermore, in neither transient nor stagnation point elongational flows is saturation observed for this PS.

Poly(ethylene oxide) versus *polystyrene*. The differences between stagnation point and transient elongational flow of PS solutions are observed in *Figure 20*. The stagnation point flow has a transition to a deformed coil at a lower strain rate, and has a larger absolute birefringence. However, in neither type of flow was saturation observed. The results for the stagnation point elongational flow of PS solutions are contrary to those reported by Odell and Keller[30], where birefringence saturation was observed. This could be due to the lower

‡The absence of a maximum in the birefringence intensity at the stagnation point is likely due to the large size of the focused beam relative to the coil dimensions. Therefore, the observed birefringence signal is due to a combination of the signals of chains at the stagnation point as well as chains on streamlines near the stagnation point. For the latter, the polymer chains continue to accelerate as they move toward the orifice and further extend. This is an explanation for the observed trend which shows the 'volume average' birefringence signal increasing toward the orifice even though, at the molecular level, the maximum chain extension for any single chain occurs at the stagnation point

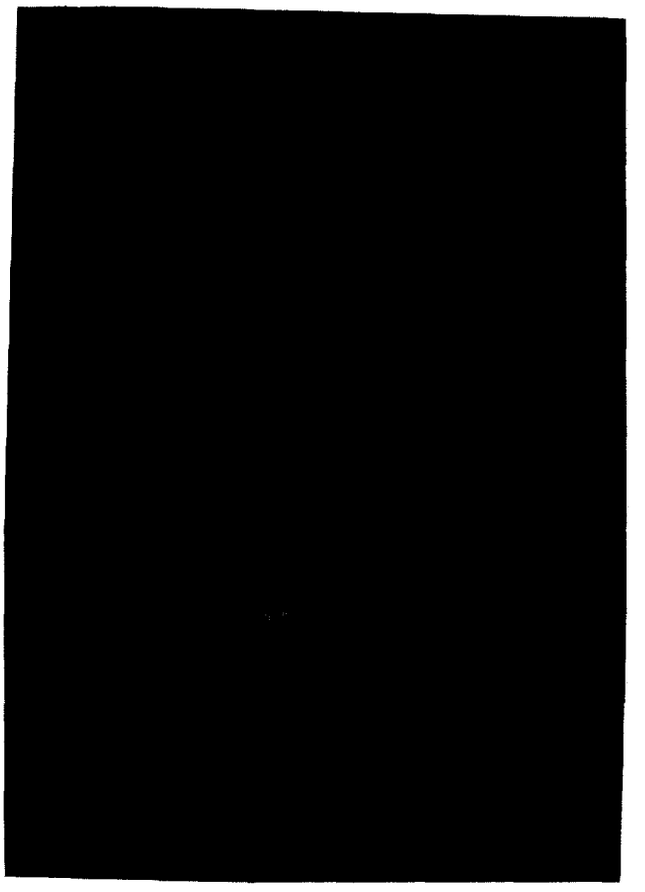

Figure 17 Optical photograph of a 1000 ppm solution of PS in decalin with a molecular weight of 4.00×10^6. This stagnation point elongational flow experiment was performed at a strain rate of $7.55 \times 10^4\ s^{-1}$ and recorded on 3000 ASA Polaroid film with an exposure time of 1.0 s. The narrow birefringent 'line' is clearly observable between the two jets

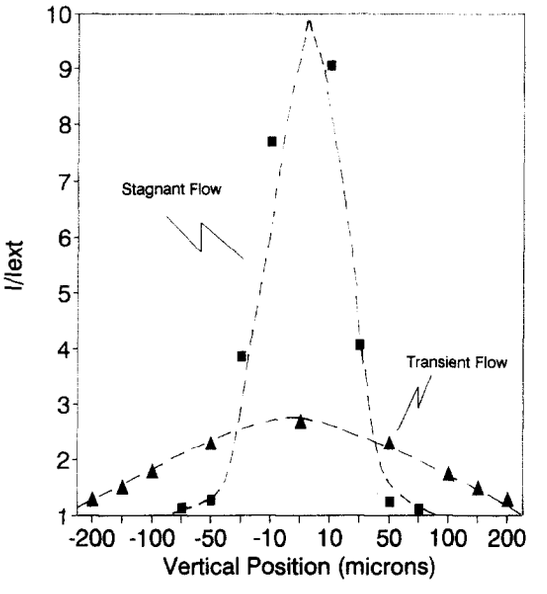

Figure 18 Birefringence intensity profiles (I), scaled with respect to the birefringence intensity at extinction (I_{EXT}), are plotted as a function of the vertical distance from the centre of the orifice. Measurements were performed on a 1000.0 ppm solution of PS with a molecular weight of 4.00×10^6 dissolved in decalin. Two profiles are shown corresponding to measurements in stagnation point (■) and transient elongational flow fields (▲). The profiles were recorded at a flow rate of 85.7 ml min^{-1} and a strain rate of $3.18 \times 10^4\ s^{-1}$. The vertical position corresponds to the distance above and below the centre of the flow axis. This centre symmetry point corresponds to the midpoint of the jet orifice

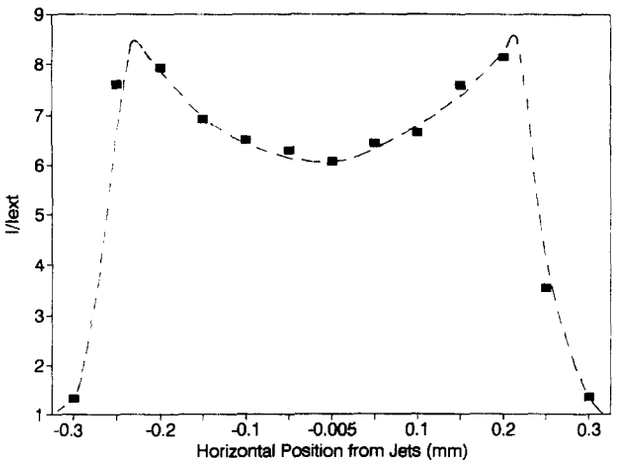

Figure 19 The birefringence intensity (I), scaled with respect to the birefringence intensity at extinction (I_{EXT}), is plotted as a function of the horizontal distance (mm) from the midpoint of the opposed jets. Experiments were performed on a PS solution with a molecular weight of 4.00×10^6 in a stagnation point flow apparatus. Polymers were dissolved in decalin at a concentration of 1000 ppm

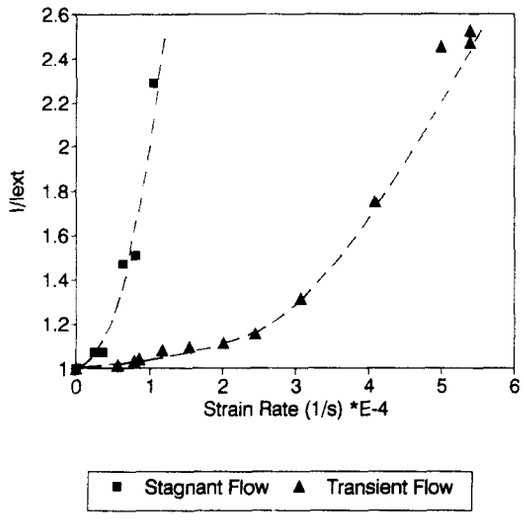

Figure 20 Birefringence intensity measurements (I), scaled with respect to the birefringence intensity at extinction at intensity (I_{EXT}), are plotted as a function of the applied strain rate (ϵ). Data are for a PS with a molecular weight of 4.00×10^6 daltons dissolved in decalin at a concentration of 1000 ppm. The data do not show a significant difference between the onset of coil deformation in transient (▲) and stagnation point (■) elongational flows

molecular weight PS samples used herein (higher molecular weights employed by Odell and Keller may be easier to saturate, particularly over an experimentally attainable strain or flow rate) or differences in the geometry employed.

The birefringence-strain rate data (*Figures 10* and *20*) also indicate that $\tau_{PEO} \sim 3\tau_{PS}$ which implies that PEO is more expanded in aqueous solution than PS in decalin. Odell and Keller[30] have reported an essentially identical relationship between $\dot{\epsilon}_{c-s,PEO}$ and $\dot{\epsilon}_{c-s,PS}$. These data are not important *per se*, since radius of gyration measurements are a more precise tool by which to measure molecular sizes. However, the agreement between the critical strain rate data and the static dimensions lends some support to the ability to make molecular inferences about isolated polymer chains based on observations under dynamic conditions.

Chain degradation. It is interesting to correlate the vertical birefringent profiles of *Figure 18* with observations of chain degradation. The latter indicate that fracture is much more efficient in transient flows (up to 80% for a single pass) compared with stagnation point elongational flow fields (less than 0.5%). Furthermore, in transient flows the critical strain rate for fracture also has a different molecular weight scaling law, with $\dot{\epsilon}_f \propto M^{-1}$ vs $\dot{\epsilon}_f \propto M^{-2}$ in quasi-stationary state flows. It therefore appears that in stagnation point flows the energy of the flow is transmitted to only a small fraction of the molecules passing through the jets. This would correspond to the chains on streamlines close to the stagnation point. In contrast, in a transient flow, virtually all molecules passing through the orifice are extended to a somewhat smaller extent as is evident from the breadth of the birefringence line. If only a modest segmental deformation is necessary for fracture, then this would account for the more efficient scission in transient flows. This is shown schematically in *Figure 21*. If a minimum level of stress in the chain is required for fracture, and this scales with the birefringence intensity, then from *Figure 21* it is clear that a much larger fraction of chains in a transient flow could have acquired sufficient energy to fracture than in a stagnation point flow. This can be explained as follows.

Mechanochemical degradation is a thermochemical process where the activation energy for bond dissociation is lowered by the application of mechanical energy. Given this, a critical energy level per carbon–carbon bond which is required for bond dissociation can be calculated (dashed horizontal line in *Figure 21*). If one assumes that the energy accumulated per bond scales with the birefringence, then an energy accumulated per bond vs vertical distance plot would be very similar to a vertical birefringence profile, such as in *Figure 18*. From *Figure 18* it is therefore evident that a transient flow imparts energy to a much larger fraction of the chains passing through the orifice than a stagnation point flow which uses its energy to more highly elongate a fewer number of chains closer to the centre of the flow axis. The ratios b/d_0 and a/d_0 in *Figure 21* are related to the fraction of chains passing through the orifice which have accumulated sufficient energy per bond to degrade. (The fraction of chains degrading is defined as the number of chains which have accumulated sufficient energy to fracture. This is related to the volume of solution passing through the orifice which has gone through the strong flow region, which scales with $(b/d_0)^3$ and $(a/d_0)^3$). A much larger fraction of the chains in a transient flow have accumulated sufficient energy to fracture than stagnation point flows, and this could explain the two-order of magnitude more efficient degradation in transient flows.

The experimental results from this work, in particular the differences in the behaviour of polymer chains in stagnation point and transient elongational flows, have been compared with other literature and used to evaluate models for polymer chain dynamics in a companion paper[31].

ACKNOWLEDGEMENTS

Support of this research by the Swiss National Science Foundation is gratefully acknowledged. One of the authors (DH) would also like to thank the EPFL for

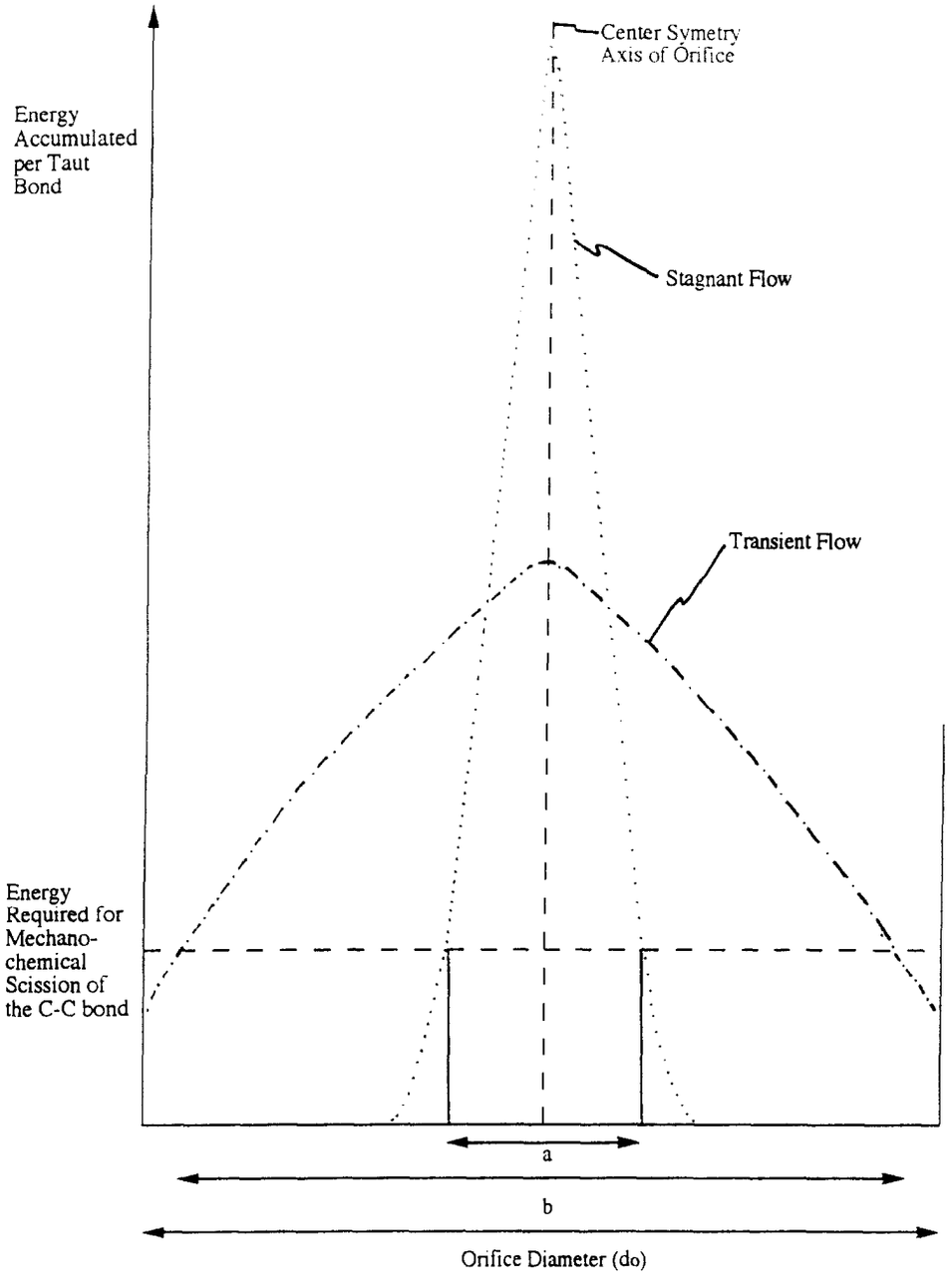

Figure 21 The energy accumulated per taut bond is plotted as a function of the vertical position from the symmetry centre of the flow axis. This is a schematic of the vertical profiles of *Figure 18* and is constructed to explain the fracture behaviour of elongational flows. (- - - -), Calculated critical energy level per carbon-carbon bond required for bond dissociation; (-.-.-), energy accumulated per taut bond for transient elongational flows; (.....), energy accumulated per taut bond for stagnation point elongational flows; a, region where chains in a stagnation point elongational flow field have an energy level greater than that required for bond scission; b, region where chains in a transient elongational flow field have an energy level greater than that required for bond scission

financial support, and HHK and TQN for all their efforts in making this collaboration possible.

REFERENCES

1 de Gennes, P. G. *J. Chem. Phys.* 1974, **60,** 5030
2 Keller, A. and Odell, J. A. *Colloid Polym. Sci.* 1985, **263,** 181
3 Frank, F. C., Keller, A. and Macley, M. R. *Polymer* 1971 **12,** 467
4 Marrucci, G. *Polym. Eng. Sci.* 1975, **15,** 229
5 Muller, A. J. PhD Thesis, University of Bristol, 1989
6 Rabin, Y. and Ottinger, H. C. *Europhys. Lett.* 1990, **13,** 423
7 Larson, R. G. *Rheol. Acta* 1990, **29,** 371
8 Ryskin, G. *J. Fluid Mech.* 1987, **178,** 423
9 Daoudi, S. *J. Phys. Paris Lett.* 1976, **37,** 241
10 Hinch, E. J.*Phys. Fluids* 1977, **20,** 522
11 De Gennes, P. G. 'Scaling Concepts in Polymer Physics', Cornell University Press, Ithaca, NY, 1979
12 Nguyen, T. Q., Yu, G. and Kausch, H. H. MACROAKRON '94 Proceedings, Akron, OH, 11–15 July, 1994, p. 892; submitted to *Macromolecules*
13 Nguyen, T. Q. and Kausch, H. H. *Adv. Polym. Sci.* 1992, **100,** 73
14 Farrell, C. J., Keller, A., Miles, M. J. and Pope, D. *Polymer* 1980, **21,** 1292
15 Lessec, J. Institute Pierre et Marie Curie, Paris, France. Distributed by Waters/Millipore
16 Cathey, C. A. and Fuller, G. G. *J. Non-Newtonian Fluid Mech.* 1990, **34,** 63
17 Fujita, H. 'Polymer Solutions', Elsevier, Amsterdam, 1990, p. 182
18 Hasegawa, T. and Nakamura, H. *J. Non-Newtonian Fluid Mech.* 1991, **38,** 159

19 Krämer, U. and Hoffmann, H. *Macromolecules* 1991, **24,** 256
20 Keller, A., Odell, J. A. and Miles, M. J. *Polymer* 1985, **26,** 1219
21 Armstrong, R. C., Gupta, S. K. and Basaran, O. *Polym. Eng. Sci.* 1980, **20,** 466
22 Menasveta, M. J. and Hoagland, D. A. *Macromolecules* 1991, **24,** 3427
23 Mackey, M. R. and Keller, A. *Phil. Trans. Roy. Soc. London* 1975, **A278,** 29: Pope, D. P. and Keller, A. *Coll. Polym. Sci.* 1978, **256,** 751
24 Farinato, R. S. *Polymer* 1988, **29,** 2182
25 Chow, A., Keller, A., Müller, A. J. and Odell, J. A. *Macromolecules* 1988, **21,** 250
26 Pogodina, N. V., Yelampieva, N. P., Lazareva, M. A., Zakharov, V. I. and Tsvetkov, V. N. *Vysokomol. soyed.* 1989, **A31,** 1070
27 Klenin, S. I., Lyubina, S. Ya., Baranovskaya, I. A., Bykova, Ye. N., Makogon, B. P. and Molotkov, V. A. *Vysokomol. soyed.* 1990, **A32,** 439.
28 Peterlin, A. *Kolloid-Z. Z. Polym.* 1963, **187,** 68
29 Smith, K. A., Merrill, E. W., Peebles, L. H. and Banijamali, S. H. in 'Polymeres et Lubrification', Colloques Internationaux du CNRS, Paris No. 233, 1975, p. 341
30 Odell, J. A. and Keller, A. *J. Polym. Sci., Polym. Phys. Edn.* 1986, **24,** 1889
31 Hunkeler, D., Nguyen, T. Q. and Kausch, H. H. *Polymer* 1996, **37,** 4271
32 Atkins, E. D. T., Attwool, P. T. and Miles, M. J. unpublished data
33 Kirkwood, J. G. and Riseman, J. *J. Chem. Phys.* 1948, **16,** 565
34 Zimm, B. H. *J. Chem. Phys.* 1956, **24,** 269
35 Nguyen, T. Q. and Kausch, H. H. *J. Non-Newtonian Fluid Mech.* 1988, **30,** 125
36 Nguyen, T. Q. and Kausch, H. H. *Macromolecules* 1990, **23,** 5137